ISSN 1606-867X (Print)
ISSN 2687-0711 (Online)
Конденсированные среды и межфазные границы
https://journals.vsu.ru/kcmf/

Оригинальные статьи

Научная статья
https://doi.org/10.17308/kcmf.2025.27/12811

The potential corrosion inhibition properties of acetyl benzoic acid derivatives with substituted alkali metals (Na, K, Li): DFT approach

R. O. Kareem[1]✉, O. A. Hamad[2]

[1]Physics Department, College of Science, University of Halabja, Halabja 46018, Iraq

[2]University of Raparin, College of Science, Department of Chemistry, Sulamani 46012, Iraq

Abstract

Purpose: Inhibitors of corrosion shield metals from corroding. Such chemicals may be added to a corrosive environment to either halt or slow down metal corrosion. The molecular structure of 3-acetyl benzoic acid (3ABA) $C_9H_8O_3$ consists of planar molecules. These molecules aggregate by centrosymmetric hydrogen-bond pairing of ordered carboxyl groups. The novelty of the research and its primary objective was to perform a theoretical computational study on derivatives of 3ABA-M (Metal), where M molecule is modified by adding lithium (Li), sodium (Na), and potassium (K).

Experimental part: The study was carried out withing the framework of the density functional theory (DFT) at the B3LYP/6-31G+ (d) level in the Gaussian 09W software. It involved geometrical optimization, analyzing spectral properties, electronic transitions, and the energy gap between the Highest Occupied Molecular Orbital (HOMO) and Lowest Unoccupied Molecular Orbital (LUMO). The calculated properties included E_{HOMO}, E_{LUMO}, energy band gap (Egap), ionization energy (IE), electron affinity (EA), absolute electronegativity (χ), global hardness (η), and global softness (S).

Conclusions: The chemical reactivity of the studied molecule was investigated by analyzing its molecular electrostatic potential (MEP) and electron localization function (ELF), using the Multiwfn 3.7 software. Consequently, it was concluded that the large energy gap of 3BAB (5.617 eV) and its high hardness (2.809) correlate with a low refractive index, dielectric constant, and low corrosion inhibition, whereas significant molecular softness of 3ABA-Na (2.88 eV^{-1}) is associated with a high refractive index.

Keywords: 3-Acetyl Benzoic Acid, Corrosion Inhibition, DFT, Electron Localized Function, Refractive Index

Acknowledgements: We express our gratitude to the leaders of Department of physics, college of Science & Halabja University.

Для цитирования: Карим Р. О., Хамад О. А. Потенциальные свойства ингибирования коррозии производных ацетилбензойной кислоты с замещенными щелочными металлами (Na, K, Li): DFT подход. *Конденсированные среды и межфазные границы*. 2025;27(2): 226–236. https://doi.org/10.17308/kcmf.2025.27/12811

For citation: Kareem R. O., Hamad O. A. The potential corrosion inhibition properties of acetyl benzoic acid derivatives with substituted alkali metals (Na, K, Li): DFT approach. *Condensed Matter and Interphases.* 2025;27(2): 226–236. https://doi.org/10.17308/kcmf.2025.27/12811

✉ Kareem R. O, e-mail: rebaz.kareem@uoh.edu.iq

1. Introduction

Metals can be protected from corrosion by corrosion inhibitors. Introducing such chemicals into a corrosive environment can prevent or slow down metal corrosion. One of the most popular and successful methods for protecting metal surfaces from oxidation or damage is the use of corrosion inhibitors. Every year, substantial amounts of material are lost due to corrosion and the irreversible breakdown of metals and alloys in a variety of sectors [1–4].

The global community has seen the fast spread of infectious illnesses, which pose a significant threat to human health due to the emergence of resistance to existing antimicrobial agents [5, 6]. Extensive research has been conducted on the biological properties of 3-acetylbenzoic acid (3ABA) combined with physiologically active heterocycles. It is highly valuable in the production of heterocyclic compounds and serves as a primary substance in a variety of chemical processes [7]. Due to its powerful antimicrobial capabilities, this molecule has been the focus of considerable research exploring its biological and physiological effects, including antifungal, anti-inflammatory, antibacterial, antimalarial, and anticancer effects. 3ABA is used as a component in hair dyes and as an intermediate agent in the pharmaceutical, cosmetics, agricultural, and food industries [8]. Due to its ability to effectively interact with molecular targets, the designated chemical has a diverse range of binding interactions, making it potentially valuable in the field of drug development. Fig. 1 shows the 3ABA structure with doped substituted alkali metals, lithium (Li), sodium (Na), and potassium (K).

In the past few decades, there has been a growing interest in predicting and understanding the mechanisms of interaction and adsorption between organic analytes and active substrates, particularly metals. The adsorption orientation and binding sites of 3ABA on metals were determined using Raman and SERS spectroscopy [9,10]. The findings were interpreted using quantum chemical calculations based on density functional theory (DFT) at the B3LYP/LANL2DZ level, while the absorption spectra were analyzed using the IEFPCM method across four distinct solvents. It is essential to perform DFT calculations in order to comprehend the structure of molecules and their properties. In this study, the structure, spectra, and characteristics of physiologically significant molecules were examined using hybrid functionals, including B3LYP and M062X [11,12]. The primary objective of quantum molecular DFT computations is to identify the structure geometry with the lowest value of global potential energy surface (PES).

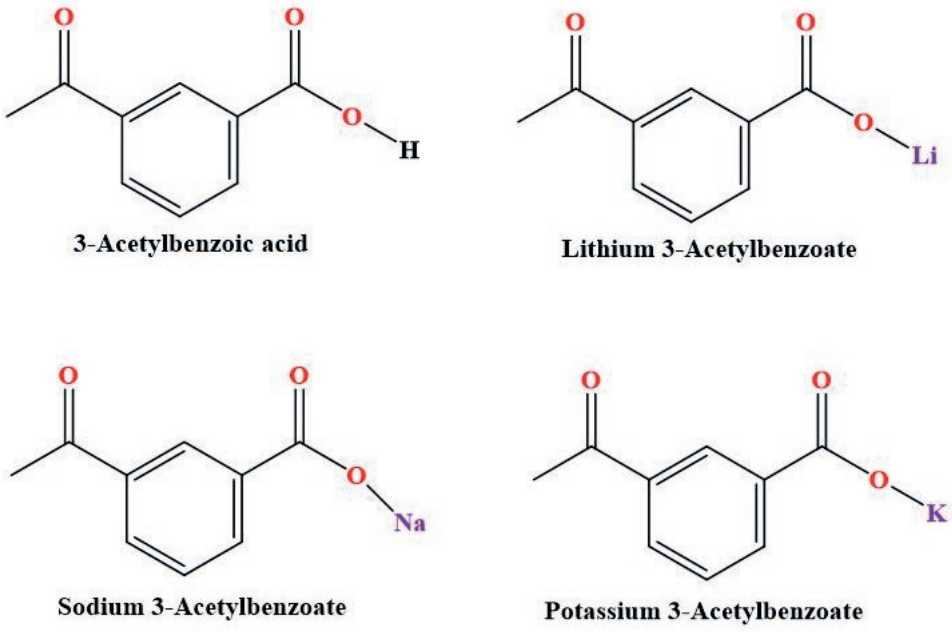

Fig. 1. 3-Acetylbenzoic acid derivative structure using Chemdraw

The experimental findings were substantiated by molecular optimization and various chemical reactivity calculations, which were used to verify the molecular behavior of the 3ABA. The spectroscopic analysis of 3ABA was used to measure its structural properties, and the results were compared to the calculated values.

The main focus of the current investigation was the structural and electronic characteristics of compounds determined through DFT calculations using the B3LYP functional and the 6-31G+(d) basis set. The acquired data made it possible to estimate the corrosion-inhibiting activity of the 3-acetylbenzoic acid (3ABA) molecule, which was examined using the Gaussian 09W software suite. In this study, zinc was substituted with alkali metals, lithium (Li), sodium (Na), and potassium (K).

2. Computational method

The molecular structure of the 3-acetylbenzoic acid (3ABA) molecule was examined using the Gaussian 09W software suite, with zinc substituted by alkali metals, lithium (Li), sodium (Na), and potassium (K). 3ABA molecule was optimized using the DFT method with the B3LYP functional and the 6-31G+(d) basis set [13]. The obtained characteristics included E_{HOMO}, E_{LUMO}, energy band gap (Eg), ionization energy (IE), electron affinity (EA), absolute electronegativity (χ), global hardness (η), and global softness (S). In addition, the molecular electrostatic potential (MEP) on the surfaces was studied [14]. The fundamental optical properties were calculated for every chemical, including work function (Φ), Fermi energy (Ef), and optical electronegativity ($\Delta\chi^*$). The electron localization function (ELF) and localized orbital locator (LOL) topologies for the studied compounds were generated using the Multiwfn 3.7 software [15].

3. Results and discussion

Quantum chemical calculations, such as the HOMO-LUMO energy analysis, are increasingly used to predict corrosion inhibition efficiency. These calculations show that the inhibitor has the ability to both donate (HOMO) and receive (LUMO) electrons from the metal surface, which affects the formation of protective layers and, eventually, the efficiency of corrosion inhibition [16, 17].

All theoretical calculations were performed using the Gaussian 09W software package, and the results were subsequently analyzed with Gaussian to evaluate them. The stability of the molecular structure was evaluated by PES scan analysis using the B3LYP level of theory with the 6-31G+(d) basis set. The electronic properties, vibrational characteristics, and optimized structures in both solid and solvation (DMSO) phase were calculated using the DFT-B3LYP method with the 6-31G+(d,p) basis set [18]. The HOMO and LUMO molecular orbitals (MOs) of an organic molecule are closely linked to its chemical and biological activities. The ground-state minimum energies of the optimized molecular structure are shown in Table 1. The energy of a bonded structure, such as an atomic unit, can be negative if the total energy of the system is lower than the sum of the energies of its individual components [19, 20].

The electrostatic potential (ESP) map simultaneously shows the molecular size, shape, and electrostatic potential using color grading, making it a great tool for correlating the chemical structures of biomolecules with their physical characteristics. According to the color coding, areas with a low electron density are shown in blue, areas with a high electron density are shown in red, and sections with no electrical charge are shown in green. The potential values decrease in the order: red < orange < yellow < green < blue. In the 3ABA-Na molecule, the most electronegative areas were located around the oxygen atoms, as shown in Fig. 2, whereas the most electron-rich regions were located in the orange and red regions. The 3ABA-Na molecule had a higher negative potential where the deeper red zones on an electrostatic potential map aligned with areas of high electronegativity. On the other hand, areas of low electronegativity in 3ABA were within lighter blue zones, indicating significantly more positive potential. Fig. 2 shows that the most electron-rich (red and orange) and electronegative (bright) areas of the 3ABA- molecule are centered around the oxygen atoms; while other electron-rich (yellow) areas are at the centers of the cyclopentadienyl rings of ferrocene and the benzene rings, where negatively charged carbon atoms are present [21].

We described the optimized bond lengths and angles for the studied molecule, 3-acetylbenzoic acid, in two distinct phases: gas phase and solvation phase. The experimental data for the studied molecule were then compared with the results from the theoretical optimization of its structure. The studied molecule consists of thirteen carbon atoms, eight hydrogen atoms, and three oxygen atoms (Fig. 2). Bond lengths and bond angles associated with the bonds connected to O1 and O2 in the original structure are notably short. These bonds exhibit the shortest bonds recorded both experimentally and theoretically. The bond angles with the smallest values are C12-O2-H20, C10-C11-H17, and O2-C12-C6 while O1-C10, O3-C12, and O2-C12 are the shortest bonds. C4-C10 and C4-C7-H14 are bond angles with the greatest values, whereas C4-C7-C9 and C10-C11 are the longest bonds [22].

3.1. HOMO–LUMO analysis

Molecular electrostatic potential analysis provides a good visualization of the reactivity of molecules identifying sites prone to nucleophilic or electrophilic attack. The studied molecule contains the following components: a benzene ring, a carbonyl group, a carboxyl group, and a methyl group. The electrostatic potentials are shown using various colors. Specifically, a deep red color indicates a negative potential, which implies nucleophilic attack. Conversely, a bright blue color signifies a positive potential, representing an electrophilic attack. Finally, a green color represents a zero potential, indicating a radical attack. As can be seen from the figure, nucleophilic attack in the molecule is most pronounced in the benzene ring attached to the carboxyl group, as well as in the benzene and methyl groups attached to the carbonyl groups. Conversely, the electrophilic attack is observed in the methyl group and benzene ring. Alternatively, the chemical behavior of the 3ABA molecule may be characterized by calculating its HOMO-LUMO energies. These energies are shown in Fig. 3. The HOMO-LUMO energies calculated for 3ABA, 3ABA–Li, 3ABA–Na, and 3ABA–K in the gas system are: –7.12805, –4.89915, –4.71835, and –4.59419 eV and –1.51103, –1.04438, –1.25094, and –1.12211 eV respectively. The band energy gaps for these compounds are: 5.617, 3.855, 3.467, and 3.472 eV respectively. The studied molecule exhibits a higher electrophilicity index (3.322 eV) and a higher electronegativity (4.320 eV). The results are shown in Table 1 [23]. These values provide strong evidence of the enhanced electronic transition in the studied molecule.

To characterize the molecular structure and determine the optical and electrical properties of molecules, particularly 3ABA and 3ABA-M, the potential energy map, or PEM, is crucial. The values of electronegativity for 3ABA, 3ABA - Li, 3ABA - Na, and 3ABA - K were 4.320, 2.972, 2.985, and 2.858 eV, respectively. Similarly, the values for hardness and softness were 2.809, 1.927, 1.734, and 1.736 eV and 0.178, 0.259, 0.288, and 0.288 eV, respectively. As can be seen from Table 1, this means that 3ABA is more stable and less reactive than 3ABA-M. The blue zone, corresponding to the higher electrophilicity index of 3ABA (4.320 eV), indicates areas with a higher electron density. The potential energy map can also be impacted by other factors, such as electronegativity [24].

In molecular orbital theory, the "EHOMO-ELUMO energy gap" refers to the minimum energy required to excite an electron from the highest occupied molecular orbital to the lowest unoccupied molecular orbital. This energy gap is the key indicator of the substance's chemical reactivity and stability. The 3ABA, 3ABA - Li, 3ABA - Na, and 3ABA – K compounds had the following HOMO and LUMO values: –7.12805, –4.89915, –4.7183 and –4.59419 eV and –1.51103, –1.04438, –1.25094 and –1.12211 eV respectively.

Thus, it can be concluded that a larger energy band gap indicates a softer molecule, but the opposite is also true: a greater molecular hardness 3ABA (2.809 eV) is associated with a softer molecule, as Table 1 illustrates. These results show that the neutral molecule was impacted by Li, Na, and K elements. A molecular structure with a smaller energy gap, such as the 3ABA - Na compound, exhibits increased flexibility and high polarization, which are directly linked to decreased stability and increased chemical reactivity. This means that it performs better as a corrosion inhibitor. The inhibitory efficiencies of the studied compounds follow the order: 3ABA - Na > 3ABA - K > 3ABA - Li > 3ABA >, which aligns well with the theoretical data. These data suggest that the five extremely electronegative

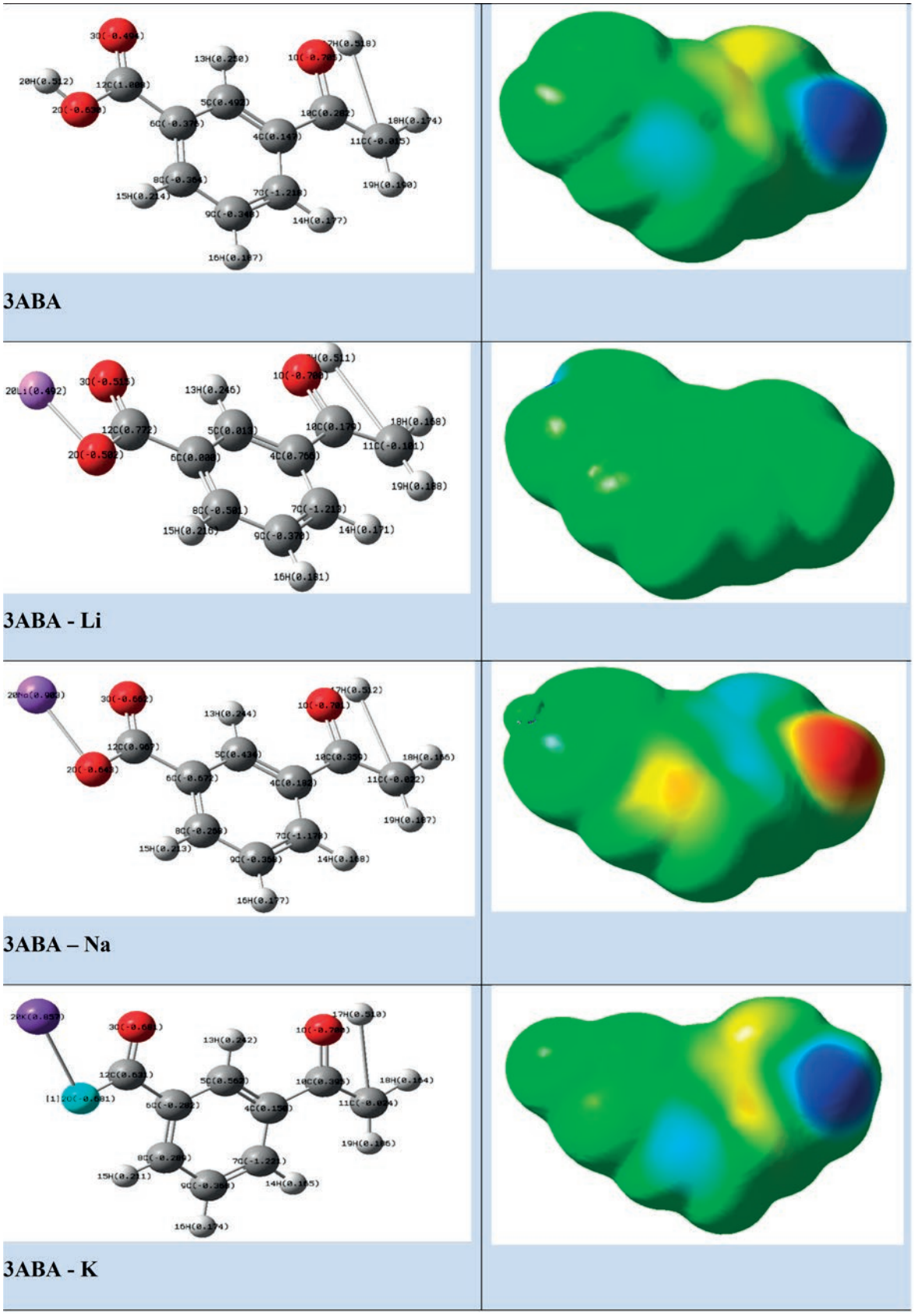

Fig. 2. Left-hand geometry optimization, right hand Electro static potential (ESP) surface

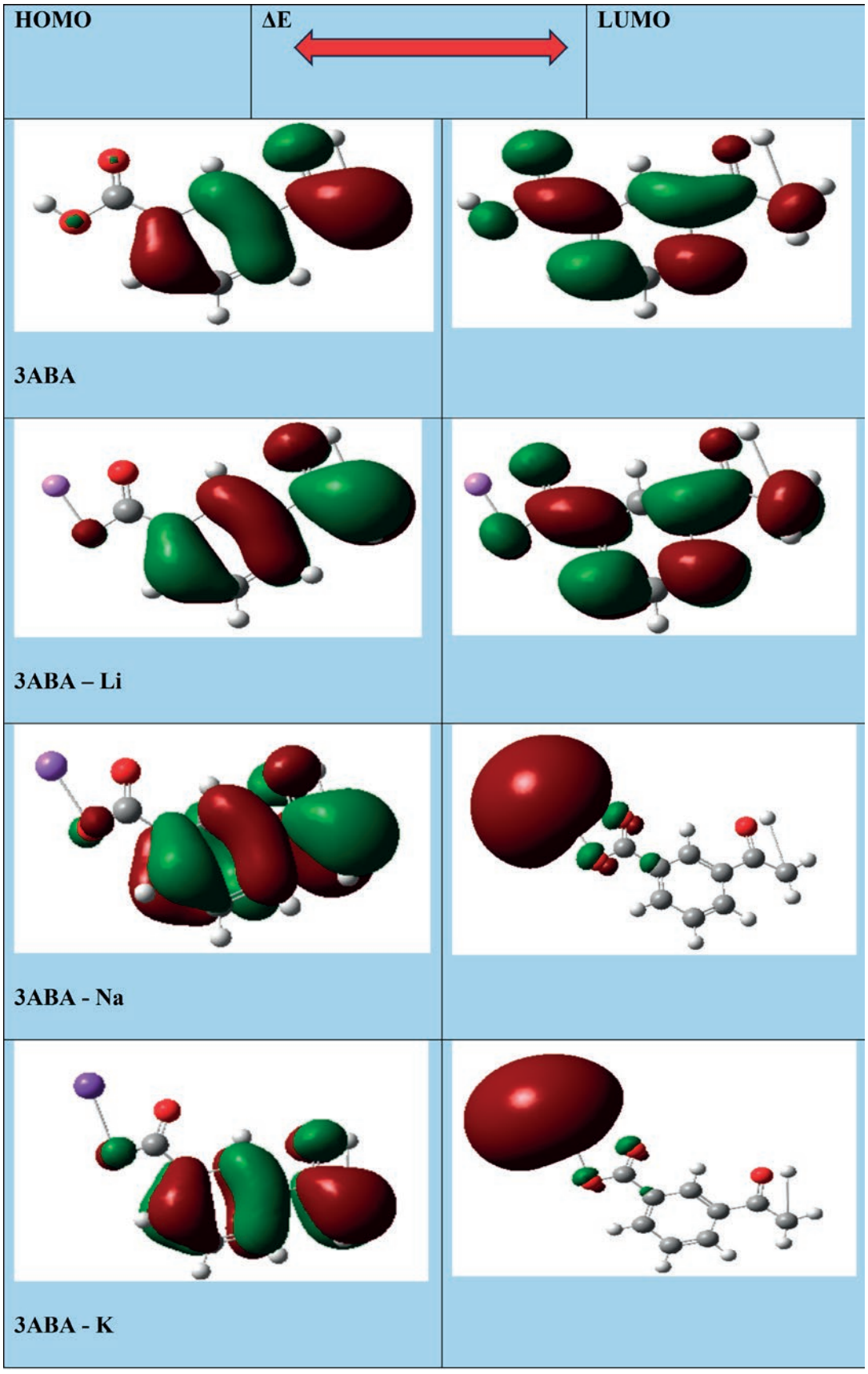

Fig. 3. The FMOS for the title compounds

Table 1. Global reactivates calculation

Parameters [25]	3ABA	3ABA - Li	3ABA - Na	3ABA - K
SCF energy (a.u)	−572.98	−508.45	−735.22	−1172.81
HOMO (eV)	−7.12805	−4.89915	−4.71835	−4.59419
LUMO (eV)	−1.51103	−1.04438	−1.25094	−1.12211
IP (eV)	7.128	4.899	4.718	4.594
EA (eV)	1.511	1.044	1.251	1.122
Band gap energy (E_g) (eV)	5.617	3.855	3.467	3.472
Hardness (η) (eV)	2.809	1.927	1.734	1.736
Softness (*S*)	0.178	0.259	0.288	0.288
Electronegativity (χ) (eV)	4.320	2.972	2.985	2.858
Chemical potential (μ) (eV)	−4.320	−2.972	−2.985	−2.858
Electrophilicity index (ω) (eV)	3.322	2.291	2.569	2.353
nucleophilicity index	0.301	0.436	0.389	0.425
back-donation	−0.702	−0.482	−0.433	−0.434
charge transfer (ΔN_{max})	1.538	1.542	1.722	1.646
Total Dipole Moment (*D*y)	7.028	5.195	6.328	9.622
Fermi level energy (E_f) (eV)	−7.884	−5.421	−5.344	−5.155
work function (Φ) (eV)	7.884	5.421	5.344	5.155
Optical electronegativity ($\Delta\chi^*$)	1.505356	1.03314	0.929156	0.930496

3ABA molecules (4.320 eV) are ineffective corrosion inhibitors. Fig 4. shows global reactivity correlations for the studied compounds.

The energy gap values, ranked from highest to lowest, are: 3ABA > 3ABA - Li > 3ABA - K > 3ABA - Na. In contrast, the refractive indices follow the opposite order: 3ABA - Na > 3ABA - K > 3ABA - Li > 3ABA. Similarly, the dielectric constants are arranged as 3ABA - Na > 3ABA - K > 3ABA – Li > 3ABA. Data from Tables 1 and 2 show a linear inverse relationship between refractive index and dielectric constant and the HOMO-LUMO energy gap. Consequently, we have revealed that a higher hardness (η) value corresponds to a lower refractive index and dielectric constant, whereas greater molecular softness (*S*) is associated with higher refractive index.

In summary, a large HOMO and LUMO energy band gap (3ABA), lower refractive index (3ABA), and dielectric constant (3ABA) indicate poor corrosion inhibition performance due to its lower electrical conductivity and reduced reactivity, while a smaller energy band gap for 3ABA – Na is associated with enhanced corrosion inhibition potential (Tables 1 and 2).

3.2. Electron localization function (ELF)

In computational chemistry, the electron localization function (ELF) is a valuable tool for visualizing and understanding the distribution of electrons within molecules. ELF provides insights into the electronic structure by indicating the probability of finding electrons localized in specific regions. There is a correlation between the ELF and the likelihood of electrons with the

Table 2. Refractive indexes of compounds (*n*), and Dielectric constants of computed (ε)

Calculated Methods	6-31G (d,p)							
	Refractive indexes (n)				Dielectric constants of computed (ε)			
	3ABA	3ABA - Li	3ABA - Na	3ABA - K	3ABA	3ABA - Li	3ABA - Na	3ABA - K
Moss Relation [26]	2.027	2.228	2.287	2.287	4.112	4.964	5.234	5.230
Ravind Revelation [27]	0.601	1.693	1.934	1.931	0.361	2.868	3.741	3.729
Herve Relation [27]	1.799	2.108	2.200	2.199	3.239	4.447	4.843	4.838
Reddy relation [28]	2.327	2.577	2.654	2.653	5.414	6.642	7.045	7.040
Kumar Relation [29]	1.930	2.179	2.255	2.254	3.726	4.749	5.085	5.080
Tripathy Relation [29]	1.889	2.141	2.237	2.236	3.569	4.587	5.007	5.001

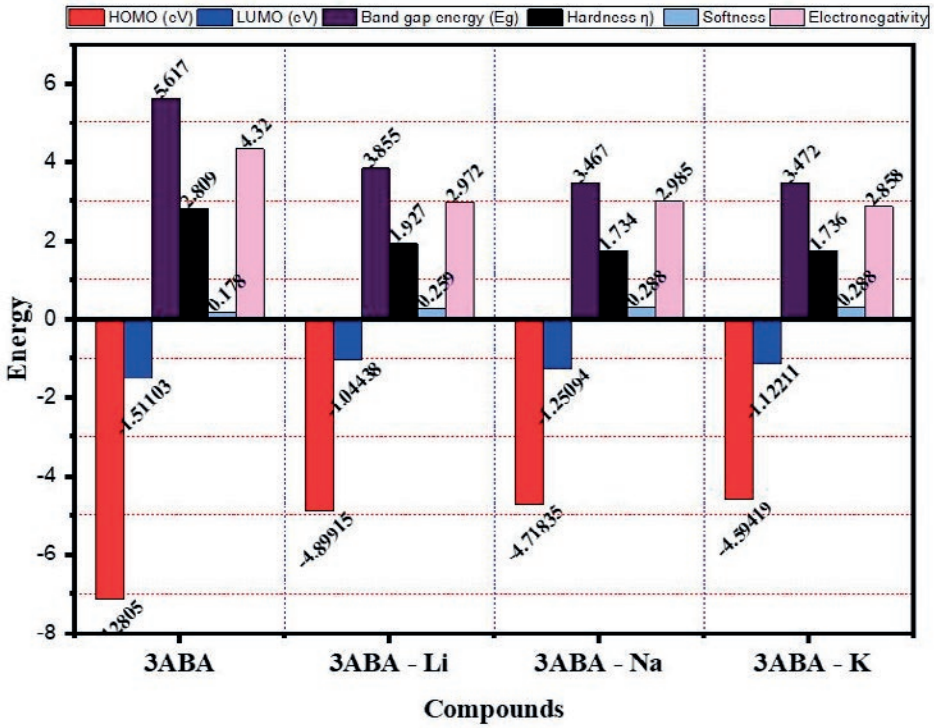

Fig. 4. The global reactivity correlations

same spin being close to each other. This method identifies regions of electron pairing, including bonds, lone pairs, and core electrons. The ELF values range from zero to one, where 0 indicates completely delocalized electrons and 1 stands for highly localized electrons.

Important characteristics: regions near atomic nuclei exhibit high ELF values (close to 1), indicating localized core electrons. In bonding regions, ELF values are intermediate, reflecting the sharing of electron pairs between atoms. High ELF values in areas that are not engaged in bonding correspond to lone pairs.

A related concept, LOL, is concerned with the localization of orbitals rather than electron pairs. Based on the kinetic energy density, LOL helps identify regions with concentrated electron density. LOL provides a complementary perspective to ELF, making it particularly useful for analyzing the kinetic aspects of electron localization.

Important characteristics of bonding and non-bonding regions: LOL highlights the probable locations of electrons in both bonding and non-bonding orbitals. It can provide a more accurate view of orbital localization than ELF, especially in complex systems, and can be useful for visualization purposes.

In this study an ELF shaded surface map was used in computational chemistry to show where electrons were located within a molecule. This three-dimensional map enables chemists to better understand bonding patterns, lone pairs, and core electrons. The use of a color scale enhances visualization, clearly highlighting the nature of chemical bonds and interactions. Fig. 5 shows an ELF color-filled map with a color scale ranging from 0.000 to 1.000. The blue surface represents delocalized electrons (below 0.500) around the carbon and oxygen atoms, whereas the red surface indicates highly localized electrons (over 0.500) around the hydrogen atoms. Covalent bond interactions are indicated by the red area between C-C atoms, while the blue areas correspond to electron depletion zones between shells [22].

4. Conclusion

In conclusion, our extensive investigation employing Gaussian simulations with DFT approach, using the B3LYP functional and 6-31G+(d) basis set, provided valuable insights into the molecular properties of 3-acetyl benzoic acid (3ABA) $C_9H_8O_3$. The primary objective of this research was to theoretical study derivatives

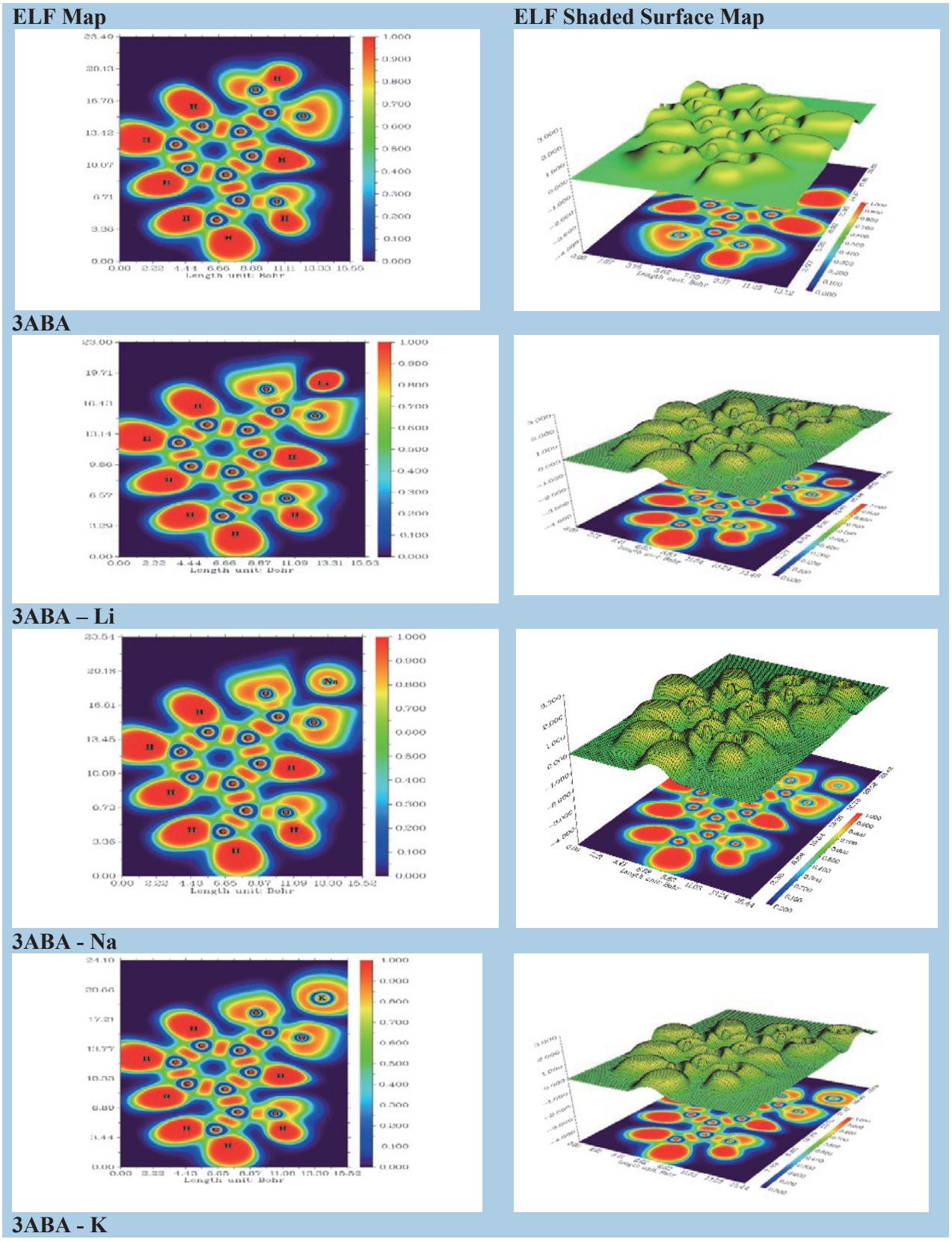

Fig. 5. The ELF, and ELF shaded surface map

of 3ABA-M (Metal) where M is represented by lithium (Li), sodium (Na), and potassium (K). The analysis revealed that the most electron-rich (red and orange) and electronegative (bright) areas of the 3ABA molecule are located near the oxygen atoms; while other electron-rich (yellow) areas are found in the center of the cyclopentadienyl rings of ferrocene and benzene rings, where negatively charged carbon atoms are present. A molecular structure with a smaller energy gap, such as the 3ABA - Na compound (3.467 eV), along with lower hardness (1.734 eV) and higher softness (0.288 eV^{-1}) has enhanced flexibility and high polarization. These properties are associated with decreased stability and increased chemical reactivity, which contribute to its superior performance as a corrosion inhibitor. Consequently, it can be concluded that a large energy gap in 3ABA (5.617 eV) and a high hardness (2.809eV) correspond to low refractive index and dielectric constant values, whereas significant molecular softness of 3ABA-Na (2.88 eV^{-1}) is associated with a higher refractive index. In the ELF color-filled map, the blue surface represents delocalized electrons (below 0.500) around the carbon and oxygen atoms, whereas the red surface indicates highly localized electrons (over 0.500) around the hydrogen atoms.

The online version contains supplementary material.

Contribution of the authors

Kareem R. O. – idea, text writing, scientific editing of the text, and Software; Hamad O. A. – search and analysis of literary data, text writing.

Conflict of interests

The authors declare that they have no known competing financial interests or personal relationships that could have influenced the work reported in this paper.

References

1. Verma C., Ebenso E. E, Quraishi M., Hussain C. M. Recent developments in sustainable corrosion inhibitors: design, performance and industrial scale applications. *Materials Advances*. 2021;2(12): 3806–3850. https://doi.org/10.1039/D0MA00681E

2. Aslam R., Serdaroglu G., Zehra S., ... Quraishi M. Corrosion inhibition of steel using different families of organic compounds: Past and present progress. *Journal of Molecular Liquids*. 2022;348: 118373. https://doi.org/10.1016/j.molliq.2021.118373

3. Verma C., Chauhan D. S., Aslam R., ...Dubey S. Principles and theories of green chemistry for corrosion science and engineering: design and application. *Green Chemistry*. 2024;26(8): 4270–4357. https://doi.org/10.1039/D3GC05207A

4. Mazumder M. J. Global impact of corrosion: occurrence, cost and mitigation. *Glob Journal Engineer Science*. 2020;5(4): 1–5. https://doi.org/10.33552/GJES.2020.05.000618

5. Pittman C. U., Stahl G. A. Copolymerization of pentachlorophenyl acrylate with vinyl acetate and ethyl acrylate. Polymer-bound fungicides. *Journal of Applied Polymer Science*. 1981;26(7): 2403–2413. https://doi.org/10.1002/app.1981.070260726

6. Apostol T.-V., Chifiriuc M. C., Draghici C., ... Barbuceanu S.-F. Synthesis, in silico and in vitro evaluation of antimicrobial and toxicity features of new 4-[(4-chlorophenyl) sulfonyl] benzoic acid derivatives. *Molecules*. 2021;26(16): 5107. https://doi.org/10.3390/molecules26165107

7. Park E.-S., Moon W.-S., Song M.-J., Kim M.-N., Chung K.-H., Yoon J.-S. Antimicrobial activity of phenol and benzoic acid derivatives. *International Biodeterioration & Biodegradation*. 2001;47(4): 209–214. https://doi.org/10.1016/S0964-8305(01)00058-0

8. Parc H. W., Park E. H., Yun H. M., Rhim H. Sodium benzoate-mediated cytotoxicity in mammalian cells. *Journal of Food Biochemistry*. 2011;35(4): 1034–1046. https://doi.org/10.1111/j.1745-4514.2010.00432.x

9. Thirumurugan P., Matosiuk D., Jozwiak K. Click chemistry for drug development and diverse chemical–biology applications. *Chemical Reviews*. 2013;113(7): 4905–4979. https://doi.org/10.1021/cr200409f

10. Ayankojo A. G., Reut J., Nguyen V. B. C., Boroznjak R., Syritski V. Advances in detection of antibiotic pollutants in aqueous media using molecular imprinting technique – a review. *Biosensors*. 2022;12(7): 441. https://doi.org/10.3390/bios12070441

11. Maier T. M., Arbuznikov A. V., Kaupp M. Local hybrid functionals: theory, implementation, and performance of an emerging new tool in quantum chemistry and beyond. *WIREs Computational Molecular Science*. 2019;9(1): 1378. https://doi.org/10.1002/wcms.1378

12. Ghalla H., Issaoui N., Govindarajan M., Flakus H., Jamroz M., Oujia B. Spectroscopic and molecular structure investigation of 2-furanacrylic acid monomer and dimer using HF and DFT methods. *Journal of Molecular Structure*. 2014;1059: 132–143. https://doi.org/10.1016/j.molstruc.2013.11.037

13. Azeez Y. H., Kareem R. O., Qader A. F., Omer R. A., Ahmed L. O. Spectroscopic characteristics, stability, reactivity, and corrosion inhibition of ahpe-dop compounds incorporating (B, Fe, Ga, Ti): a DFT investigation. *Next Materials*. 2024;3: 100184. https://doi.org/10.1016/j.nxmate.2024.100184

14. Kareem R. O., Kebiroglu H., Hamad O. A. Investigation of electronic and spectroscopic properties of phosphosilicate glass molecule (BioGlass 45S5) and Ti-BioGlass 45S5 by quantum programming. *Journal of Chemistry Letters*. 2024;4(4): 200–210. https://doi.org/10.22034/

jchemlett.2024.416584.1138

15. Shukla S., Srivastava A., Kumar P., Tandon P., Maurya R., Singh R. Vibrational spectroscopic, NBO, AIM, and multiwfn study of tectorigenin: a DFT approach. *Journal of Molecular Structure*. 2020;1217: 128443. https://doi.org/10.1016/j.molstruc.2020.128443

16. Nadr R. B., Abdulrahman B. S., Azeez Y. H., Omer R. A., Kareem R.O. Quantum chemical calculation for synthesis some thiazolidin-4-one derivatives. *Journal of Molecular Structure*. 2024;1308: 138055. https://doi.org/10.1016/j.molstruc.2024.138055

17. Mamand D. M., Azeez Y. H., Qadr H. M. Monte Carlo and DFT calculations on the corrosion inhibition efficiency of some benzimide molecules. *Mongolian Journal of Chemistry*. 2023;24(50): 1–10. https://doi.org/10.5564/mjc.v24i50.2435

18. Azeez Y. H., Kareem R. O., Hamad O., ... Kaygılı O. Quantum chemical calculation employed for investigation mesitylene compound. *Journal of Physical Chemistry and Functional Materials*. 2024;7(1): 17–27. https://doi.org/10.54565/jphcfum.1350445

19. Issaoui N., Abdessalem K., Ghalla H., Yaghmour S. J., Calvo F., Oujia B. Theoretical investigation of the relative stability of Na+Hen (n = 2–24) clusters: Many-body versus delocalization effects. *The Journal of Chemical Physics*. 2014;141(17). https://doi.org/10.1063/1.4900873

20. Gong Y. Structure-property relationships of dyes as applied to dye-sensitized solar cells. 2018. *Repository*. https://doi.org/10.17863/CAM.22164

21. Raja M., Muhamed R. R., Muthu S., Suresh M. Synthesis, spectroscopic (FT-IR, FT-Raman, NMR, UV–Visible), NLO, NBO, HOMO-LUMO, Fukui function and molecular docking study of (E)-1-(5-bromo-2-hydroxybenzylidene)semicarbazide. *Journal of Molecular Structure*. 2017;1141: 284–298. https://doi.org/10.1016/j.molstruc.2017.03.117

22. Vijayakumari G., Iyandurai N., Raja M., ... Muthu S. Chemical reactivity, solvent effects, spectroscopic (FTIR, Raman, SERS, UV–Visible), Hirshfeld analyses and antimalarial investigation of 3-Acetylbenzoic acid. *Chemical Physics Impact*. 2023;6: 100190. https://doi.org/10.1016/j.chphi.2023.100190

23. Mohammed B. A., Kareem R. O., Hamad O. A., Kebiroglu H. The electronic structure and physicochemical characteristics of chlorohydroquinone compounds using density functional theory and Hartree-Fock techniques. *South African Journal Chemistry*. 2024;78: 85–94. https://doi.org/10.17159/0379-4350/2024/v78a12

24. Kareem R. O., Hanifi Kebiroğlu M., Hamad O. A. H., Kaygili O., Bulut N. Epinephrine compound: unveiling its optical and thermochemical properties via quantum computation methods. https://doi.org/10.2139/ssrn.4603446

25. Hamad O., Kareem R. O., Kaygılı O. Density function theory study of the physicochemical characteristics of 2-nitrophenol. *Journal of Physical Chemistry and Functional Materials*. 2023;6(1): 70–76. https://doi.org/10.54565/jphcfum.1273771

26. Moss T. A relationship between the refractive index and the Infra-Red threshold of sensitivity for photoconductors. *Proceedings of the Physical Society Section B*. 1950;63(3): 167. https://doi.org/10.1088/0370-1301/63/3/302

27. Ravindra N., Auluck S., Srivastava V. On the penn gap in semiconductors. *Physica Status Solidi (b)*. 1979;93(2): K155–K160. https://doi.org/10.1002/pssb.2220930257

28. Reddy R., Gopal K. R., Narasimhulu K., ... Kumar M. R. Interrelationship between structural, optical, electronic and elastic properties of materials. *Journal of Alloys and Compounds*. 2009;473(1-2): 28–35. https://doi.org/10.1016/j.jallcom.2008.06.037

29. Kumar V., Singh J. Model for calculating the refractive index of different materials. *NIScPR Online Periodicals Repository*. 2010;48(08): 571–574.

Information about the authors

Rebaz Obaid Kareem, M.Sc in General Physics, Lecturer at the Departmet of Physics, Faculty of Science, Physics Department, Halabja University (Kurdistan Region, Iraq).

https://orcid.org/0000-0001-6273-1309

rebaz.kareem@uoh.edi.iq

Othman Abdulrahman Hamad, PhD in Organic Chemistry, University of Raparin, College of Science, Department of Chemistry (Sulamani, Iraq).

https://orcid.org/0000-0001-8170-9094

osman20f@gmai.com

Received 03.10.2024; approved after reviewing 13.11.2024; accepted for publication 16.12.2024; published online 25.06.2025.